Structures and Properties of Stable Al_4, Al_4^+, and Al_4^- Comparatively Studied by ab Initio Theories

Y. L. Zhao*

Institute of Material Science and Engineering, Ocean University of China, Qingdao, Shandong 266100, China

R. J. Zhang

Department of Applied Physics, Chongqing University, Chongqing 400044, China

Received: February 23, 2007; In Final Form: May 11, 2007

Previous high-level theoretical calculations of aluminum clusters mostly relied on density functional theory (DFT) or theories less sophisticated than it. Here, we point out that a second-order Møller−Plesset perturbation (MP2) method is more appropriate and is the minimum level of theory in the predictions of property such as geometries, electronic structures, and IR and Raman spectra of Al_4, Al_4^+, and Al_4^- clusters. The theoretical electron affinities and ionization potentials predicted with MP2 geometries are closer to experimental ones than those by DFT. The p-electron characters and single valence state of aluminum atoms and IR and Raman spectra of the aluminum clusters were also reliably predicted by MP2 and could be based on for further experimental and theoretical studies.

Introduction

Aluminum clusters have been extensively studied because they could form functional complexes with other provided groups, exhibiting multiple characteristics such as special catalyst,[1,2] biologic activity,[3] and conductivity.[4,5] In nature, its excellent properties result from the particular bond formations and atom combinations of the clusters. Hence, the proper confirmation of the ground-state structure is crucial to give the right guidance for further explorations.

Previous studies[6−24] of aluminum clusters had been performed using semiempirical molecular orbital calculations,[6] molecular dynamics (MD),[7−9] Hartree−Fock (HF),[10] and density functional theory (DFT).[11−17] However, different theories frequently concluded different ground-state structures and gave inconsistent theoretical predictions[6,7,11,18−20] for Al_n clusters. For example, Upton[18,19] reported that the transition of the planar structures to three-dimensional (3D) ones started from $n = 4$ for Al_n clusters by configuration interaction calculations, whereas Jug et al.[6] suggested that the 3D structures are favored by the ones with more than four atoms at the level of semiempirical theory. Pettersson et al.[20] found that the dimensional transition did not emerge until $n = 6$ by using correlated wave functions and extended basis sets. Furthermore, both Jones[7] and Rao[11] have reported that the ground state structures for aluminum clusters up to 5 atoms are planar by DFT. Because Al_n clusters start to show the possibility of 3D structure from $n = 4$, in this work we focused on Al_4, Al_4^+, and Al_4^- clusters and performed a through search for the real ground-state geometries. The properties (such as electronic structures, infrared and Raman spectra) of these stable clusters were also studied.

Because a correct geometrical structure is so crucial for any description of cluster properties, the structure of global minimum must be found cautiously using a reliable theory. As a matter of fact, previous studies are not accurate enough to predict a correct cluster structure, especially for a multi-electron metal cluster, due to the insufficient inclusion of electron correlation. The energy of a system is so sensitive to the electron correlation that sometimes the order of energies could be even alternated. By far, it is known that the second-order Møller−Plesset perturbation (MP2) theory is accurate enough to account for metal clusters with acceptable computational efforts. Nevertheless, it should be noted that although MP2 includes the main electron correlation, the calculations would simultaneously bring spin contamination to a high spin system. Thus, it is unclear if the MP2 could correctly predict the energy order or not among the isomers. Accordingly, in this work, to verify the reliability of the various popularly used theories, the HF, DFT, and MP2 methods were used to comparatively study the aluminum clusters. The results would allow a systematic evaluation of the importance of electron correlation effects and the effects of spin contaminations of HF and MP2 on the eigenvalues of each isomer. Ultimately, the validity of the theoretical approaches would be evaluated and reliable properties could be predicted.

Computational Details

To compare the effect of different methods on calculated results, Al_4, Al_4^+, and Al_4^- clusters were investigated by HF, B3LYP, and MP2 approaches with the basis set of 6-311+G-(d), respectively. We also reproduced the results of ref 11 at the BPW91/LANL2DZ level of theory. The determined reliable structures were further used for single-point energy correction calculations at CCSD(T)/6-311+G(2df) level of theory. Symmetry was constrained on each studied cluster. Frequencies were calculated to obtain the zero-point energy (ZPE) of each isomer and confirm the real minimum without imaginary frequencies. All calculations were conducted with Gaussian 03W package.[25]

Results and Discussion

1. Ground-State Geometries by HF, DFT, and MP2 Methods. Table 1 illustrates the symmetry and spectroscopy

* Corresponding author. E-mail: ouylzhao@yahoo.com.cn.

10.1021/jp0715373 CCC: $37.00
Published on Web 07/12/2007

TABLE 1: Symmetry, Electronic State, and Spin Contamination of Ground State Al_4, Al_4^+, and Al_4^- Clusters

		Al_4	Al_4^+	Al_4^-
HF/6-311+G(d)	symmetry (state)	D_{3h} ($^1A_1'$)	D_{3h} ($^4A_2''$)	D_{2d} ($^6A_2$)
	$\langle S^2\rangle$	0	3.8371	8.8164
	$s(s+1)$	0	3.75	8.75
B3LYP/6-311+G(d)	symmetry (state)	D_{2h} ($^3B_{3u}$)	C_{2v} ($^2B_1$)	D_{2h} (^2A_g)
	$\langle S^2\rangle$	2.0069	0.7528	0.7610
	$s(s+1)$	2	0.75	0.75
MP2/6-311+G(d)	symmetry (state)	D_{2h} ($^3B_{3u}$)	D_{2h} (^4A_u)	D_{2h} (^2A_g)
	$\langle S^2\rangle$	2.0863	3.8182	0.8414
	$s(s+1)$	2	3.75	0.75
BPW91/LANL2DZ	symmetry (state)	D_{2h} ($^3B_{3u}$)	D_{2h} (^4A_u)	D_{2h} (^2A_g)
	$\langle S^2\rangle$	2.0066	3.7565	0.7603
	$s(s+1)$	2	3.75	0.75

state of the global minima of Al_4, Al_4^+, and Al_4^- clusters predicted using HF, B3LYP, and MP2 with 6-311+G(d) basis set, respectively. For comparisons, the previous results[11] by BPW91/LANL2DZ were also reproduced. The symmetries together with the spectroscopy states of the aluminum clusters by HF method are D_{3h} ($^1A_1'$), D_{3h} ($^4A_2'$), and D_{2d} ($^6A_2$), respectively, completely different from those by DFT and MP2. B3LYP presents results much consistent with MP2 except for the Al_4^+ cluster [C_{2v} ($^2B_1$)]. Only the MP2 and BPW91 produce the same symmetry and electronic state with D_{2h} ($^3B_{3u}$), D_{2h} (^4A_u), and D_{2h} (^2A_g), respectively.

The lowest-energy geometries of Al_4, Al_4^+, and Al_4^- clusters by various methods are presented in Figure 1a−i, where the Al−Al bond length (R) and ∠Al−Al−Al bond angle are labeled. The geometries are mostly rhombus except for some triangle or tetrahedron from HF (Figures 1a,d,g) and Tundish-like from B3LYP (Figure 1e). MP2 produced rhombus geometries similar to those by BPW91, which are labeled with italics in the parentheses, as shown in Figure 1c,f,i. It was found that the order of R values for each aluminum cluster is always $R_{HF} > R_{DFT} > R_{MP2}$. For example, the R values of Al_4 cluster are 2.779, 2.724, 2.657, and 2.622 Å by HF, BPW91, B3LYP, and MP2, respectively. The MP2 predicts the Al−Al distance most close to twice of covalent radius of Al atom (1.25 Å).[26] Although BPW91 predicts a geometrical shape similar to that of MP2, the R and bond angle by BPW91 are still to some extent different from MP2.

For systems with a spin multiplicity more than 1, there may exist spin contamination resulting from the calculations of HF and MP2. According to organic molecule calculations, the spin contamination is negligible if the value of $\langle S^2\rangle$ differs from $s(s+1)$ by less than 10%. For Al_4, Al_4^+, and Al_4^-, the values of $\langle S^2\rangle$ and $s(s+1)$ listed in Table 1 show no spin contaminations from DFT, but a relatively small deviation from $s(s+1)$ for $\langle S^2\rangle$ by HF and MP2. The $\langle S^2\rangle$ values by HF/6-311+G(d) are higher than $s(s+1)$ by 2.3% and 0.76%, respectively, whereas the $\langle S^2\rangle$ by MP2/6-311+G(d) for Al_4 ($^3B_{3u}$), Al_4^+ (^4A_u), and Al_4^- (^2A_g) are respectively 4.3%, 1.8%, and 12% higher than $s(s+1)$. Although the higher spin contamination of Al_4^- from MP2 may result in the energy disorder, the problem was avoided by using its geometry at MP2/6-311+G* followed by the single point energy corrections on the high level of CCSD(T)/6-311+G(2df). Moreover, the spin contamination is not severe,

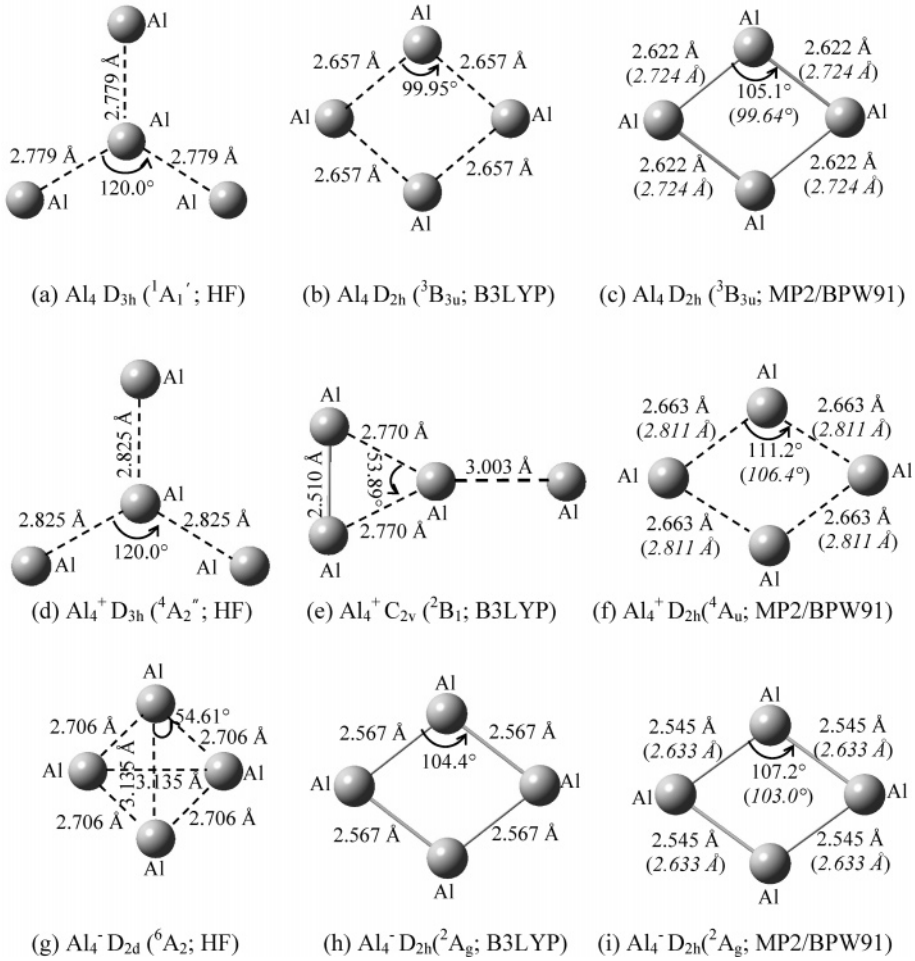

(a) Al_4 D_{3h} ($^1A_1'$; HF) (b) Al_4 D_{2h} ($^3B_{3u}$; B3LYP) (c) Al_4 D_{2h} ($^3B_{3u}$; MP2/BPW91)

(d) Al_4^+ D_{3h} ($^4A_2''$; HF) (e) Al_4^+ C_{2v} ($^2B_1$; B3LYP) (f) Al_4^+ D_{2h}(^4A_u; MP2/BPW91)

(g) Al_4^- D_{2d} ($^6A_2$; HF) (h) Al_4^- D_{2h}(^2A_g; B3LYP) (i) Al_4^- D_{2h}(^2A_g; MP2/BPW91)

Figure 1. (a)−(i) Optimized structures, symmetry, and their electronic states of Al_4, Al_4^+, and Al_4^- clusters on the level of HF, B3LYP, and MP2 with basis set 6-311+G(d). The italic values in parentheses are the BPW91/LANL2DZ results.

TABLE 2: First IP and EA (eV) of Ground State Al_4, Al_4^+, Al_4^- Clusters

transition		symmetry (state) transition	CCSD(T)/6-311+G(2df)//MP2/6-311+G(d)	BPW91/LANL2DZ	experiment
IP ($Al_4 \rightarrow Al_4^+$)	IP_v	D_{2h} ($^3B_{3u}$) → D_{2h} ($^2B_{3u}$)	6.68	6.69	~6.55[27]
		D_{2h} ($^3B_{3u}$) → D_{2h} (^4A_u)	6.44	6.58	
	IP_a	D_{2h} ($^3B_{3u}$) → D_{2h} (^4A_u)	6.38	6.50	
EA ($Al_4^- \rightarrow Al_4$)	EA_v	D_{2h} (^2A_g) → D_{2h} (^1A_g)	3.32	3.42	3.35[28]
		D_{2h} (^2A_g) → D_{2h} ($^3B_{3u}$)	2.33	2.19	2.25[28]
	EA_a	D_{2h} (^2A_g) → D_{2h} ($^3B_{3u}$)	2.24	2.13	2.20 ± 0.05[29]

as most deviations were found to be small, not beyond the 10% limit. Overall, the results predicted by MP2 are reliable and useful.

2. Ionization Potential (IP) and Electron Affinities (EA). The adiabatic IP (IP_a) for $Al_4 \rightarrow Al_4^+$ was obtained by calculating the energy difference (ΔE) between the ground state structures of Al_4^+ and Al_4, and the vertical IP (IP_v) for $Al_4 \rightarrow Al_4^+$ was obtained from ΔE between Al_4^+ and Al_4 with the same geometry of the latter. Similarly, the adiabatic EA (EA_a) and vertical EA (EA_v) potential for $Al_4^- \rightarrow Al_4$ were also obtained. For more accurate IP and EA values, single energy corrections were performed at the level of CCSD(T)/6-311+G-(2df) on the basis of the lowest-energy structures by MP2/6-311+G(d). The IP and EA results from CCSD(T), BPW91 and experiments are respectively listed in Table 2. The results by CCSD(T)/6-311+G(2df) are closer to experiments than BPW91/LANL2DZ, confirming a better geometrical reliability of MP2 than DFT. For example, the average IP_v value from CCSD for $Al_4 \rightarrow Al_4^+$ at the multiplicities of 2 (6.68 eV) and 4 (6.44 eV) is 6.56 eV, nearly equal to the experimental value, 6.55 eV,[27] but the average IP_v value by BPW91 is 6.64 eV, 0.09 eV higher than experiments. Moreover, the EA_v for $Al_4^-(^2A_g) \rightarrow Al_4(^1A_g)$ is 3.32 eV from CCSD and 3.42 eV by BPW91, only 0.9% difference, but 2.1% difference from the experimental value (3.35 eV),[28] respectively. Although the EA_v for $Al_4^-(^2A_g) \rightarrow Al_4(^3B_{3u})$ by CCSD (2.33 eV) deviates more than that by BPW91 (2.19 eV) from the experimental one (2.25 eV), the EA_v values by BPW91 are too high or too low because the difference (1.23 eV) of EA_v values by BPW91 between the two

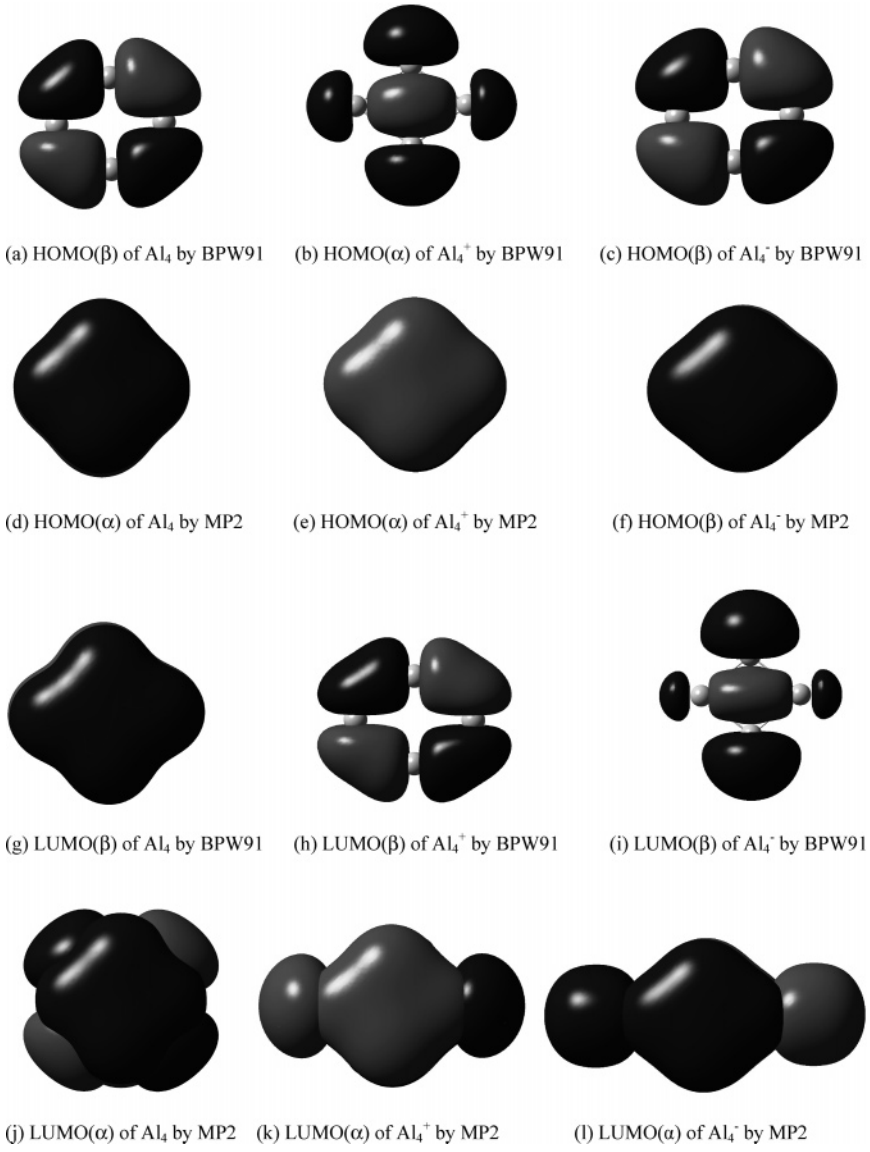

Figure 2. Frontier molecular orbitals of Al_4, Al_4^+, and Al_4^- at the levels of BPW91/LANL2DZ and MP2/6-311+G(d).

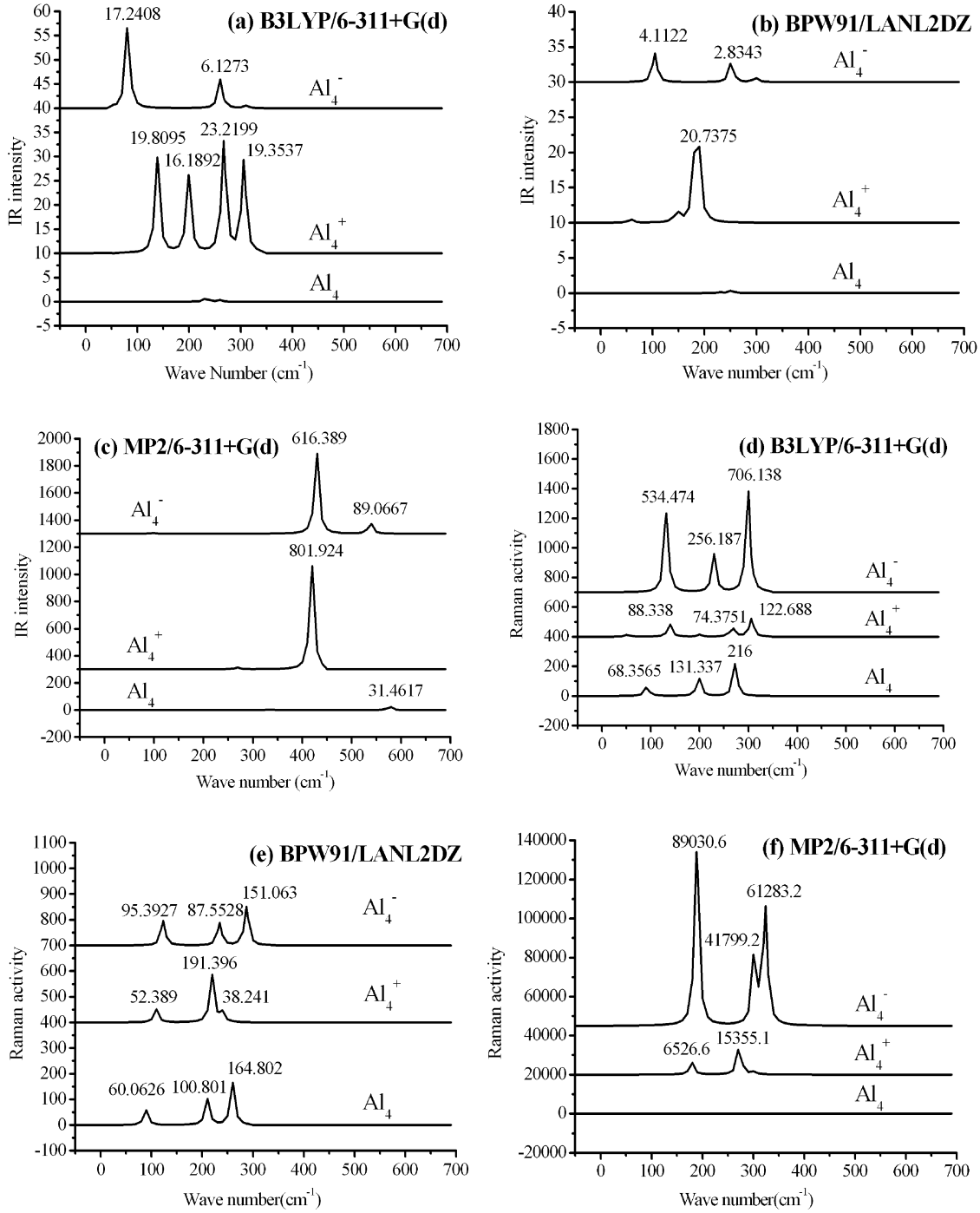

Figure 3. IR spectra of Al_4, Al_4^+, and Al_4^- clusters at the levels of and Raman spectra of Al_4, Al_4^+, and Al_4^- clusters at the levels of B3LYP/6-311+G(d), BPW91/LANL2DZ, and MP2/6-311+G(d).

multiplicities is much larger than that (0.99 eV) by CCSD correction. The latter is slightly more reasonable and closer to the difference by experiments (1.10 eV). Thus, our IP and EA results could further support that the MP2 geometries are more reliable than those of DFT.

3. Frontier Molecular Orbitals by HF, DFT. and MP2. HOMO and LUMO contours could provide an intuitionist understanding of their electronic structures. Due to the great geometry difference, the frontier molecular orbitals (FMOs) by HF are abnormal and thus omitted to show here. The FMO contours of the clusters (of similar shapes) from BPW91 and MP2 are comparatively illustrated in Figure 2a−l. It is noted that the orbitals labeled MP2 in Figure 2 are HF ones using the MP2 geometries. It is shown that there is p-electron conjugation to some extent in BPW91 calculation, whereas, obviously, the HOMO and LUMO patterns of the aluminum cluster by MP2 all present correctly the p-electron conjugation, as the outmost electronic layer of small aluminum clusters mainly consists of 3p electron due to the large 3p−3s energy separation.[29] The FMO figures should be p-like conjugation and single valence property. Only the results by MP2 are qualified to well present such an orbital feature.

4. IR and Raman Spectra by B3LYP, BPW91, and MP2. Figure 3 shows the IR intensities and Raman activities of each aluminum cluster by B3LYP, BPW91, and MP2. The IR and Raman spectra are respectively depicted in the range of 0−700 cm^{-1}. There are six vibrational modes corresponding to five stretching vibrational modes and one bending vibrational mode.

The dipole moment or polarizability changes are responsible to IR intensities or Raman activities.

Obvious discrepancies are found between the IR/Raman peak values predicted by DFT and MP2 methods. By MP2/6-311+G(d), the IR intensities of Al_4^+ and Al_4^- are as large as 801.924 at 418.824 cm^{-1} and 616.389 at 428.934 cm^{-1}, respectively, much higher than that of Al_4, only 31.4617 at 576.835 cm^{-1}. However, the DFT results could not give evidently different IR intensities, although the tendency is still $Al_4^+ > Al_4^- > Al_4$. For instance, by B3LYP/6-311+G(d), the highest IR intensities of Al_4^+ and Al_4^- are only 23.2199 at 266.849 cm^{-1} and 17.2408 at 81.0533 cm^{-1}, respectively, and that of Al_4 is nearly zero. Similarly, by BPW91/LANL2DZ, the high peaks of Al_4^+ and Al_4^- appear as 20.7375 at 185.199 cm^{-1} and 4.1122 at 104.180 cm^{-1}, respectively. The IR intensity of Al_4 is about zero, too. Thus, MP2 provided wider and higher peak values of IR intensities for aluminum clusters than DFT, although the trend of intensity change is similar.

The order of Raman activity predicted by MP2 is $Al_4^- > Al_4^+ > Al_4$. As shown in Figure 3f, the Raman spectrum of Al_4^- involves three peaks with high activities of 89030.6 at 188.291 cm^{-1}, 41799.2 at 302.438 cm^{-1}, and 61283.2 at 323.822 cm^{-1}, respectively, due to large changes of polarizabilities associated with the stretching vibrations. As for Al_4^+, there also exist three peaks with relatively high activities, being 6526.60 at 178.566 cm^{-1}, 15355.1 at 272.322 cm^{-1}, and 1523.37 at 302.420 cm^{-1}. Only Al_4 exhibits small Raman activity, 281.606 and 39.3289 at 295.703 and 170.794 cm^{-1}, respectively. Due to the strong Raman activity contrast among Al_4, Al_4^+, and Al_4^-, some small peaks predicted by MP2/6-311+G(d) even could not appear in Figure 3f. Such a large difference of Raman activities among the aluminum clusters could provide the fingerprint and confirmation clue for experimentalists.

Conclusions

Through the systematic study of the Al_4, Al_4^+, and Al_4^- clusters by HF, B3LYP, BPW91, and MP2, we confirm that it is MP2 rather than DFT that is the adequate method for the prediction of aluminum cluster geometries and properties. The validity and superiority of MP2 theory are verified by calculating IP and EA values which are very close to the experimental ones. The FMO patterns of Al_4, Al_4^+, and Al_4^- by MP2 present correctly the p-electron conjugation. MP2 predicted more obvious contrast in the peak values of IR and Raman spectra for aluminum clusters than DFT. Owing to the reliable MP2 geometries, MP2 calculations could provide reliable fingerprint and confirmation clue for experimentalists. Moreover, our work could provide reliable theory guidance for studying other Al_n clusters.

References and Notes

(1) Anand, R.; Maheswari, R.; Hanefeld, U. *J. Catal.* **2006**, *242*, 82.
(2) Jermy, B. R.; Pandurangan, A. *J. Mol. Catal. A: Chem.* **2006**, *256*, 184.
(3) Ferraro, G. A.; Perrotta, A.; Rossano, F.; Andrea, F. D. *Aesth. Plast. Surg.* **2004**, *28*, 431.
(4) Lavrinaitis, M. V.; Gruznev, D. V.; Tsukanov, D. A.; Ryzhkov, S. V. *Tech. Phys. Lett.* **2005**, *31*, 1068.
(5) Yamamura, H.; Matsusita, T.; Nishino, H.; Kakinuma, K. *J. Mater. Sci.: Mater. Electron.* **2002**, *13*, 57.
(6) Jug, K.; Schluff, H. P.; Kupka, H.; Iffert, R. *J. Comput. Chem.* **1988**, *9*, 803.
(7) Jones, R. O. *J. Chem. Phys.* **1993**, *99*, 1194.
(8) Akola, J.; Manninen, M.; Häkkinen, H.; Landman, U.; Li, X.; Wang, L. S. *Phys. Rev. B* **1999**, *60*, 11297.
(9) Lloyd, L. D.; Johnston, R. L. *Chem. Phys.* **1998**, *236*, 107.
(10) Ueno, J.; Hoshino, T.; Hata, M.; Tsuda, M. *Appl. Surf. Sci.* **2000**, *162−163*, 440.
(11) Rao, B. K.; Jena, P. *J. Chem. Phys.* **1999**, *111*, 1890.
(12) Cheng, H. P.; Berry, R. S.; Whetten, R. L. *Phys. Rev. B* **1991**, *43*, 10647.
(13) Yi, J. Y.; Oh, D. J.; Bernhole, J. *Phys. Rev. Lett.* **1991**, *67*, 1594.
(14) Akola, J.; Häkkinen, H.; Manninen, M. *Phys. Rev. B* **1998**, *58*, 3601.
(15) Ahlrichs, R.; Elliott, S. D. *Phys. Chem. Chem. Phys.* **1999**, *1*, 13.
(16) Khanna, S. N.; Jena, P. *Phys. Rev. Lett.* **1992**, *69*, 1664.
(17) Gong, X. G.; Kumar, V. *Phys. Rev. Lett.* **1993**, *70*, 2078.
(18) Upton, T. H. *Phys. Rev. Lett.* **1986**, *56*, 2168.
(19) Upton, T. H. *J. Chem. Phys.* **1987**, *86*, 7054.
(20) Pettersson, L. G. M.; Bauschlicher, C. W.; Halicioglu, T., Jr. *J. Chem. Phys.* **1987**, *87*, 2205.
(21) Schultz, N. E.; Staszewska, G.; Staszewski, P.; Truhlar, D. G. *J. Phys. Chem. B* **2004**, *108*, 4850.
(22) Cha, C. Y.; Ganteför, G.; Eberhardt, W. *J. Chem. Phys.* **1994**, *100*, 995.
(23) Martínez, A.; Vela, A.; Salahub, D. R.; Calaminici, P.; Russo, N. *J. Chem. Phys.* **1994**, *101*, 10677.
(24) Zhan, C. G.; Zheng, F.; Dixon, D. A. *J. Am. Chem. Soc.* **2002**, *124*, 14795.
(25) Frisch, M. J.; Trucks, G. W.; Schlegel, H. B.; Scuseria, G. E.; Robb, M. A.; Cheeseman, J. R.; Zakrzewski, V. G.; Montgomery, J. A., Jr.; Stratmann, R. E.; Burant, J. C.; Dapprich, S.; Millam, J. M.; Daniels, A. D.; Kudin, K. N.; Strain, M. C.; Farkas, O.; Tomasi, J.; Barone, V.; Cossi, M.; Cammi, R.; Mennucci, B.; Pomelli, C.; Adamo, C; Clifford, S.; Ochterski, J.; Petersson, G. A.; Ayala, P. Y.; Cui, Q.; Morokuma, K.; Malick, D. K.; Rabuck, A. D.; Raghavachari, K.; Foresman, J. B.; Cioslowski, J.; Ortiz, J. V.; Baboul, A. G.; Stefanov, B. B.; Liu, G.; Liashenko, A.; Piskorz, P.; Komaromi, I.; Gomperts, R.; Martin, R. L.; Fox, D. J.; Keith, T.; Al-Laham, M. A.; Peng, C. Y.; Nanayakkara, A.; Gonzalez, C.; Challacombe, M.; Gill, P. M. W.; Johnson, B.; Chen, W.; Wong, M. W.; Andres, J. L.; Gonzalez, C.; Head-Gordon, M.; Replogle, E. S.; Pople, J. A. *Gaussian 03*, revision B.05; Gaussian, Inc.: Pittsburgh, PA, 2003.
(26) Downs, A. J. *Chemistry of aluminum, gallium, indium and thallium*, 1st ed.; 1993.
(27) Schriver, K. E.; Persson, J. L.; Honea, E. C.; Whetten, R. L. *Phys. Rev. Lett.* **1990**, *64*, 2539.
(28) Taylor, K. J.; Pettiette, C. L.; Graycraft, M. J.; Chesnovsky, O.; Smalley, R. E. *Chem. Phys. Lett.* **1988**, *152*, 347.
(29) Li, X.; Wu, H. B.; Wang, X. B.; Wang, L. S. *Phys. Rev. Lett.* **1998**, *81*, 1909.